

Decomposition of time-dependent fluorescence signals reveals codon-specific kinetics of protein synthesis

Nadin Haase¹, Wolf Holtkamp², Reinhard Lipowsky¹, Marina Rodnina² and Sophia Rudorf^{1,*}

¹Theory and Bio-Systems, Max Planck Institute of Colloids and Interfaces, Am Muehlenberg 1, 14476 Potsdam, Germany and ²Physical Biochemistry, Max Planck Institute for Biophysical Chemistry, Am Fassberg 11, 37077 Goettingen, Germany

Received May 29, 2018; Revised July 23, 2018; Editorial Decision August 01, 2018; Accepted August 03, 2018

ABSTRACT

During protein synthesis, the nascent peptide chain traverses the peptide exit tunnel of the ribosome. We monitor the co-translational movement of the nascent peptide using a fluorescent probe attached to the N-terminus of the nascent chain. Due to fluorophore quenching, the time-dependent fluorescence signal emitted by an individual peptide is determined by co-translational events, such as secondary structure formation and peptide-tunnel interactions. To obtain information on these individual events, the measured ensemble fluorescence signal has to be decomposed into position-dependent intensities. Here, we describe mRNA translation as a Markov process with specific fluorescence intensities assigned to the different states of the process. Combining the computed stochastic time evolution of the translation process with a sequence of observed ensemble fluorescence time courses, we compute the unknown position-specific intensities and obtain detailed information on the kinetics of the translation process. In particular, we find that translation of poly(U) mRNAs dramatically slows down at the fourth UUU codon. The method presented here detects subtle differences in the position-specific fluorescence intensities and thus provides a novel approach to study translation kinetics in ensemble experiments.

INTRODUCTION

During the process of translation, ribosomes synthesize proteins by decoding mRNA. Before emerging from the ribosome, a newly synthesized peptide chain has to traverse the narrow ribosomal exit tunnel. The movement of the nascent peptide chain through the exit tunnel is influenced

by the tunnel's structure and the chemical composition of the tunnel walls. The peptide exit tunnel of bacterial ribosomes has a length of around 100 Å and can cover 30–40 amino acids of an unfolded, fully-stretched nascent peptide chain (1,2). However, a nascent peptide chain may attain different conformations as it moves deeper into the tunnel. Experimental data and computer simulations support the view that smaller structures can form within the tunnel, e.g. compacted non-native states, α -helices, hairpins or even small α -helical domains (3–9). However, the mechanism of co-translational folding remains poorly understood.

Translation elongation proceeds in a non-uniform manner (10,11). In particular, mRNA secondary structure, tRNA abundance, and sequence-specific interactions between the nascent peptide and the translating ribosome can cause pauses in translation (5,7,12). These variations in translation speed are important for the regulation of gene expression and can affect the folding of proteins. Ribosome stalling by specific motifs and peptides has been investigated in great detail (13,14). In addition, Han *et al.* (15) report a sequence-independent but position-specific ribosomal pausing at the fifth codon in eukaryotes. These pauses disappear when the exit tunnel structure is modified by deletion of the loop region from ribosome protein L4, which shows that the interaction is indeed a tunnel-specific feature.

In this paper, we describe a method to monitor the vectorial motion of a fluorescently labeled nascent peptide chain through the *Escherichia coli* ribosomal peptide exit tunnel and investigate the kinetics of this process. In particular, we study the *in-vitro* synthesis of short poly-phenylalanine peptides fMetPhe_n. Each time a new codon of a poly(U) mRNA is translated, the nascent peptide becomes longer by one phenylalanine and a new tunnel segment is probed by the fluorescent label that is attached to the N-terminus of the peptide, see Figure 1 A. Conformational changes of the nascent chain, for example after peptide bond formation, as well as altered polypeptide-tunnel interactions, evoke changes of the fluorescence signal through fluorophore

*To whom correspondence should be addressed. Tel: +49 331 567 9638; Fax: +49 331 567 9602; Email: sophia.rudorf@mpikg.mpg.de

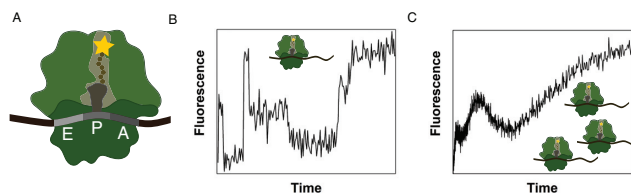


Figure 1. Fluorescence signatures of translation. (A) Ribosome (green) with P-site tRNA (dark gray) and nascent peptide chain (brown dots) in the exit tunnel (light green). The N-terminus of the nascent peptide is labeled with a fluorophore (yellow star). (B) During translation the fluorescence intensity changes because of conformational rearrangements and interactions of the nascent chain with the exit tunnel. The fluorescence signature of the synthesis of a single peptide would resemble a curve with clearly distinguishable features modulated by thermal fluctuations (schematic drawing). (C) Translation is a stochastic process. Thus, the superimposed total fluorescent signature of a large number of initially synchronized ribosomes simultaneously translating identical sequences is much smoother than each individual fluorescence time trace. Therefore, total fluorescence signatures obtained from bulk experiments have to be analytically decomposed to reveal the hidden fluorescence and kinetic information about the individual translation steps.

quenching and de-quenching. Therefore, each step of the translation process corresponds to a specific fluorescence intensity which implies that translation of an mRNA yields a time-dependent, sequence-specific fluorescence signal, see Figure 1 B. We refer to the latter signal as the *fluorescence signature* of the sequence. Translation is a stochastic process. Thus, if a large number of initially synchronized ribosomes translate identical sequences simultaneously, the superimposed total fluorescence signature exhibits less pronounced features compared to the individual signatures, see Figure 1 C. In the following, we show how total fluorescence signatures obtained from bulk experiments can be decomposed to reveal the hidden fluorescence and kinetic information about the individual translation steps.

MATERIALS AND METHODS

Computational modeling

In this subsection, we explain the decomposition of the measured fluorescence signatures of the translation process into state-dependent intensity values (IFIs). First, mRNA translation is described as a Markov process, see Figure 2 and Figures S1 to S6 in the Supplementary Information. The time evolution of the probability $P_i(t)$ to find the process in state $i = 1 \dots I$ at time t is obtained by solving the master equations

$$\frac{d}{dt} P_i(t) = \sum_{j=1}^I [(P_j(t) \omega_{ji} - P_i(t) \omega_{ij})] \quad (1)$$

where ω_{ij} denotes the rate of transitions from state i to state j (also referred to as kinetic rates). Right before initiation of translation, all ribosomes are located with their empty A site at the first codon. This corresponds to the translation process being in state 0 at time $t = 0$, i.e., the initial condition

$$P_0(0) = 1 \quad \text{and} \quad P_i(0) = 0 \quad \text{for all } i \neq 0.$$

Each translating ribosome carries exactly one fluorophore *via* the nascent peptide chain in its exit tunnel. We now assume that the superposition principle holds for the fluorescence signatures analyzed here, i.e., that the total measured fluorescence signal is simply the sum over all fluorescence intensities emitted by the individual fluorophores. Therefore, for each time point t_m , the fluorescence signature $b(t_m)$ is equal to the sum over all state-specific IFIs x_i weighted by the probabilities $P_i(t_m)$ to find a ribosome in state i at time t_m . When we combine the data from M different time points, we obtain the system of linear equations as given by

$$\mathbf{P} \vec{x} = \vec{b}(t) \quad (2)$$

with the matrix

$$\mathbf{P} = \begin{pmatrix} P_0(t_1) & P_1(t_1) & \dots & P_I(t_1) \\ P_0(t_2) & P_1(t_2) & \dots & P_I(t_2) \\ \vdots & \vdots & \ddots & \vdots \\ P_0(t_M) & P_1(t_M) & \dots & P_I(t_M) \end{pmatrix} \quad (3)$$

with I the number of states in the Markov process and M the number of measured data points. In principle, the system of equations (2) could be exactly solved for the unknown IFIs x_i . However, because of noise in the experimentally determined fluorescence signatures $b(t)$, the IFIs x_i have to be estimated simultaneously with all unknown kinetic rates ω_{ij} by a fitting procedure (see Section ‘Fluorescence signatures of poly(U) translation and their decomposition by model fitting’ for details about the fit parameters). To this end, we used MATLAB. First, we smoothed the experimental fluorescence signatures by applying a moving average with a fixed subset size. We then solved the system of equations (2) using a non-negative least-squares solver (lsqnonneg) with the IFIs x_i as adjustable parameters. The entire calculation was embedded in a for-loop that changes the unknown kinetic rates systematically between 1 and 200 s^{-1} . For each iteration, the IFIs were fitted and the predicted fluorescence signature was compared to the smoothed experimental data. The kinetic rate that produced the smallest deviation between theory and experiment in terms of least squares was taken as the best fit. The results were independent of the chosen moving average subset size within a range from 3 to 85 out of 2000 data points. All fixed parameters used in the calculation as well as detailed lists of all fitted IFIs and kinetic rates can be found in Supplementary Tables S1 to S4 in the Supplementary Information.

Experimental methods

Chemicals were purchased from Roche Molecular Biochemicals, Sigma Aldrich, or Merck. Radioactive compounds were from Hartmann Analytic. Ribosomes from *E. coli* MRE 600, BodipyFL (BOF)-Met-tRNA^{Met}, Phe-tRNA^{Phe}, EF-Tu and initiation factors were prepared as described (16–18). mRNAs were prepared by *in-vitro* transcription using Phusion polymerase (Biozym Scientific). Initiation complexes were formed in Buffer A (50 mM Tris-HCl pH 7.5, 70 mM NH₄Cl, 30 mM KCl, 7 mM MgCl₂) supplemented with DTT (1 mM) and GTP (1 mM) by incubating 70S ribosomes (0.7 μM), initiation factor IF1, 2 and

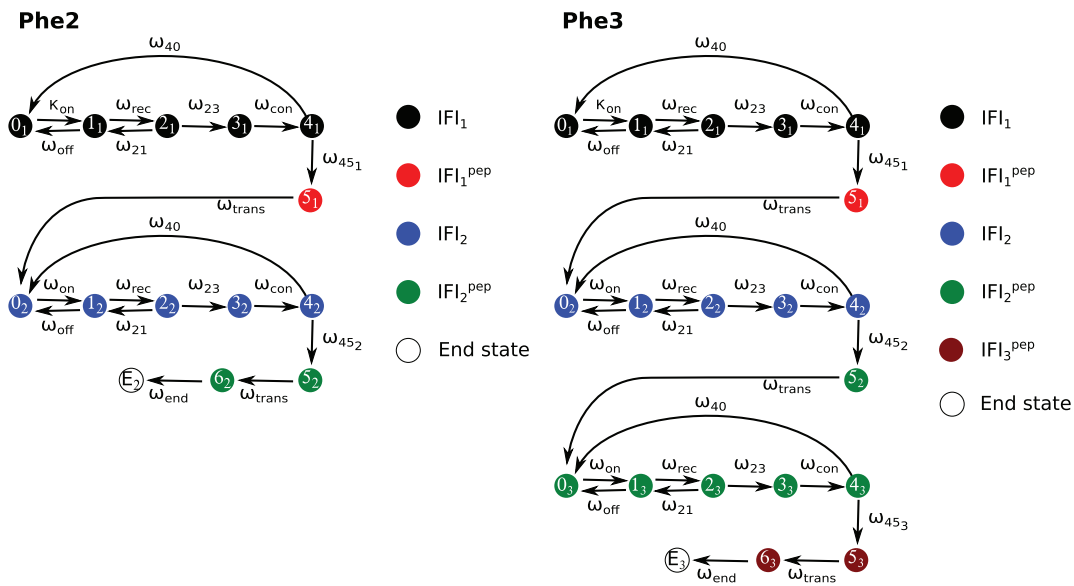


Figure 2. Representation of *phe2* and *phe3* mRNA translation as a Markov process. The transitions between different states (dots) of the Markov processes correspond to the sub-steps of the elongation cycle. The fluorescent initiation complex consisting of a ribosome with BodipyFL (BOF)-Met-tRNA^{Met} in the P site and the first UUU codon in the A site starts in state 0₁. States 0₁–4₁: Initial selection including ternary complex binding ('on'), codon reading and recognition ('rec'), GTPase activation, GTP hydrolysis and EF-Tu conformational rearrangement ('con') is followed by A-site accommodation of the first Phe-tRNA^{Phe}. After peptide bond formation (state 5₁), the ribosome translocates to the second UUU codon ('trans', state 0₂) where the same process is repeated. An alternative notation for the transition rates (k-notation) is explained in Table S1 in the Supplementary Information. In states 6₂ and 6₃ of *phe2* and *phe3* translation, respectively, the ribosomal P site is occupied by the last UUU codon of the truncated mRNA whereas the A site is empty. Finally, the trapped ribosome ends up in the end states E₂ and E₃, respectively. In principle, each state corresponds to a specific Intrinsic Fluorescence Intensity (IFI) of the light emitted by the BOF label. Dots with the same color indicate states that are assigned the same IFI to avoid overfitting.

3 (1 μM each), mRNA (2 μM) and BOF-Met-tRNA^{Met} (1.4 μM) at 37 °C for 60 min. Initiation efficiency was determined by nitrocellulose filtration and was typically 90%. All complexes were purified by centrifugation through a 1.1 M sucrose cushion in Buffer A containing 30 mM MgCl₂. Pellets were dissolved in Buffer A and tRNA binding was verified by nitrocellulose filtration. To prepare ternary complexes EF-TuGTPPhe-tRNA^{Phe}, EF-TuGTP complexes were first formed by incubating EF-Tu (40 μM) with GTP (1 mM), EF-Ts (0.02 μM), phosphoenol pyruvate (3 mM), pyruvate kinase (0.05 mg ml⁻¹) and MgCl₂ (1 mM) at 37 °C for 15 min in HiFi buffer (50 mM HEPES pH 7.5, 70 mM NH₄Cl, 30 mM KCl, 3.5 mM MgCl₂, 8 mM putrescine, 0.5 mM spermidine). The ternary complex stock solution was formed by mixing EF-TuGTP with Phe-tRNA^{Phe} (20 μM), followed by incubation for 2 min at 37 °C. Final ternary complex concentrations (10, 2, 0.3 and 0.15 μM) were achieved by dilution of the ternary complex stock solution (20 μM) with HiFi buffer. EF-G (2 μM) was supplemented or omitted as indicated. Fluorescence experiments were carried out using a stopped-flow apparatus (SX-20MV; Applied Photophysics) in HiFi buffer at 37 °C, i.e. under identical buffer conditions as in (19). BOF fluorescence was excited at 470 nm and detected after passing a KV500 cut-off filter (Schott). Equal volumes of initiation complexes (20 nM) were rapidly mixed with ternary complexes at different concentrations as indicated. Each time course is an average of at least six technical replicates.

RESULTS AND DISCUSSION

Poly(U) translation as a Markov process

We used short truncated poly(U) mRNA constructs consisting of a 5' UTR, an AUG codon, and one to five UUU codons that we refer to as *phe1*, *phe2*, ..., *phe5* depending on the number of UUU codons. Previously, we introduced a description of the translation elongation cycle as a codon-specific Markov process (19,20). Here, we investigated the *in-vitro* translation of *phe1* to *phe5* in the presence of only cognate ternary complexes. Therefore, the translation process does not involve any near- and non-cognate tRNA-ribosome interactions. Briefly, each state of the Markov process corresponds to one sub-step of the elongation cycle. Fluorescent initiation complexes consist of ribosomes with BodipyFL (BOF)-Met-tRNA^{Met} in the P site and the first UUU codon in the A site. Upon addition of the ternary complexes EF-TuGTPPhe-tRNA^{Phe}, they undergo initial selection, which entails initial binding, codon reading and recognition, GTPase activation, GTP hydrolysis and EF-Tu rearrangement, followed by aa-tRNA accommodation, peptide bond formation, and translocation to the next codon (21). The ribosomes repeat the elongation cycle until they reach the end of the truncated mRNA, thus ending up in an end state without mRNA in their A sites. As an example, Figure 2 shows the adapted Markov processes for translation of *phe2* and *phe3*. Markov representations for translation processes of longer mRNAs containing more UUU codon repeats can be found in the Supplementary Information.

Fluorescence signatures of poly(U) translation and their decomposition by model fitting

As translation proceeds, the BOF reporter attached to the N-terminus of the nascent peptide changes its fluorescence intensity depending on the environment of the exit tunnel. We monitored the change in fluorescence intensity during *in-vitro* translation of *phe1* to *phe5* mRNAs using a stopped-flow instrument, see Experimental Procedures for details. In addition, we performed an experiment where no EF-G was added to the reaction such that translation stalled after the first peptide bond has formed. The measured fluorescence signatures of the synthesis of peptides BOF-fMetPhe₁ to BOF-fMetPhe₅ as well as for the first round of decoding without EF-G are shown in Figure 3. As described in the Introduction, the measured fluorescence signatures have to be decomposed by computational methods to obtain the hidden information about the individual translation events, see Figure 1. To this end, we apply the Markov model of translation introduced in the previous paragraph.

In general, each state of the translation process should correspond to a specific value of fluorescence intensity referred to as Intrinsic Fluorescence Intensity (IFI) (22). Fitting the model to the data could reveal the state-specific IFIs as well as the kinetic rates of the process, i.e. the rates of transition between different states in the Markov model. However, given the large number of fit parameters and the limited amount of experimental data, additional constraints are necessary to avoid overfitting. First, we normalize all IFIs to the initial value and, thus, by definition the IFI of the initial state $IFI_1 = 1$. Second, we restrict the number of different IFIs. For the first codon, the experimental data suggest two changes in fluorescence: An initial change after peptide bond formation leading to IFI_1^{pep} , and a second change after translocation. The latter results in an IFI referred to as IFI_1^{trans} in case of *phe1* translation where the ribosomal A site is empty after translocation and as IFI_2 in all other cases where the A site becomes occupied by the second UUU codon after translocation, see Figure 2 and Supplementary Information. Such assignment of IFI changes is borne by the experimental data and is plausible, as the first translocation results in shifting of the BOF reporter down along the peptide exit tunnel, whereas the following translocation may result in a reorientation of the short nascent BOF-fMetPhe peptide, such that the fluorescence is altered. For all following codons, allowing more than one additional IFI per codon leads to overfitting. Therefore, only one change in fluorescence after peptide bond formation is taken into account. This again is plausible, as each subsequent peptidyl transfer event moves the BOF label down the tunnel, but with the increasing length its rotational mobility upon translocation may be restricted. The corresponding IFIs are referred to as IFI_3 , IFI_4 and IFI_5 in case the end of the mRNA has not been reached yet, and as IFI_2^{pep} to IFI_5^{pep} in case no further UUU codon follows. A final change is made when the ribosome transitions to the end state, see Figure 2. The end state formation is too slow to occur on the time scale of translation and represents a slow off-pathway rearrangement of a stalled complex. In total, there are $n + 2$ IFIs to be fitted where n is the number of UUU codons, see also Figures S1 to S6 in the Supplemen-

tary Information. As an example, translation of *phe2* and *phe3* is characterized by four and five changes in fluorescence intensity, respectively. Concerning the kinetic rates, we use values obtained in previous studies (19) and determine only the rates ω_{45_n} and ω_{trans} of peptide bond formation and translocation by fitting (see Supplementary Table S1 and S2). This is again plausible from the biochemical point of view, because the decoding process per se should depend on the codon-anticodon interaction, which should be identical for each Phe codon regardless of its position.

Implementing these constraints, we went through the following fitting procedure: First, we smoothed out short-term fluctuations in the experimental data by using a moving average. Then, data evaluation was started by analyzing of the fluorescence signature for poly(U) mRNA translation in the absence of EF-G. This analysis led to the fitted rate ω_{45_1} of peptide bond formation, which was held constant when we examined the fluorescence signature of *phe1* translation in the presence of EF-G. The latter analysis revealed the rate ω_{trans} of translocation which we kept constant during all further fitting procedures to avoid overfitting. The codon position-specific rates ω_{45_n} of peptide bond formation were obtained from the analysis of *phe2* to *phe5* translation. We also tested the alternative approach, i.e., to keep the rate ω_{45} constant during analysis of the other fluorescence signatures and to allow variation of ω_{trans} , instead. This approach led to strong deviations between fitted and experimental fluorescence signatures, which indicates that ω_{45} is a highly codon position-dependent rate rather than a constant.

Together with the $n + 2$ IFIs introduced above, there are in total $n + 2 + 1$ free fit parameters for each fluorescence signature with $n = 0$ in the absence of EF-G. Figure 3 shows the best match in terms of least squares between data and theory. The model provides a very good estimate for the experimentally observed process. This result is surprising, given that we adjust only one kinetic rate per experiment. For example, the Markov model for *phe5* translation contains 14 kinetic rates of which 13 are fixed and only one – the rate ω_{45_5} of peptide bond formation and tRNA accommodation – is fitted. Note that the positions of the peaks and dips depend only on the kinetic rates, whereas their amplitudes are determined by the IFIs. The small deviations between theoretical and experimental fluorescence signatures arise from the constraint to adjust only a single kinetic parameter for each fluorescence signature to avoid overfitting, as described above. More precisely, the accuracy of the decomposition method we describe here is limited by the trade-off between a suboptimal fit quality caused by a low number of fit parameters and the risk of overfitting that leads to ambiguous, non-interpretable fit results.

Translation dramatically slows down at the fourth codon

With all initially unknown transition rates determined by the fit procedure described above, the Markov models for *phe1* to *phe5* translation are fully parametrized. Using this information, fundamental properties of the translation process can be determined by standard techniques such as first step analysis (23). In particular, we calculated the average rate of translation for all UUU codons, see Table 1. These

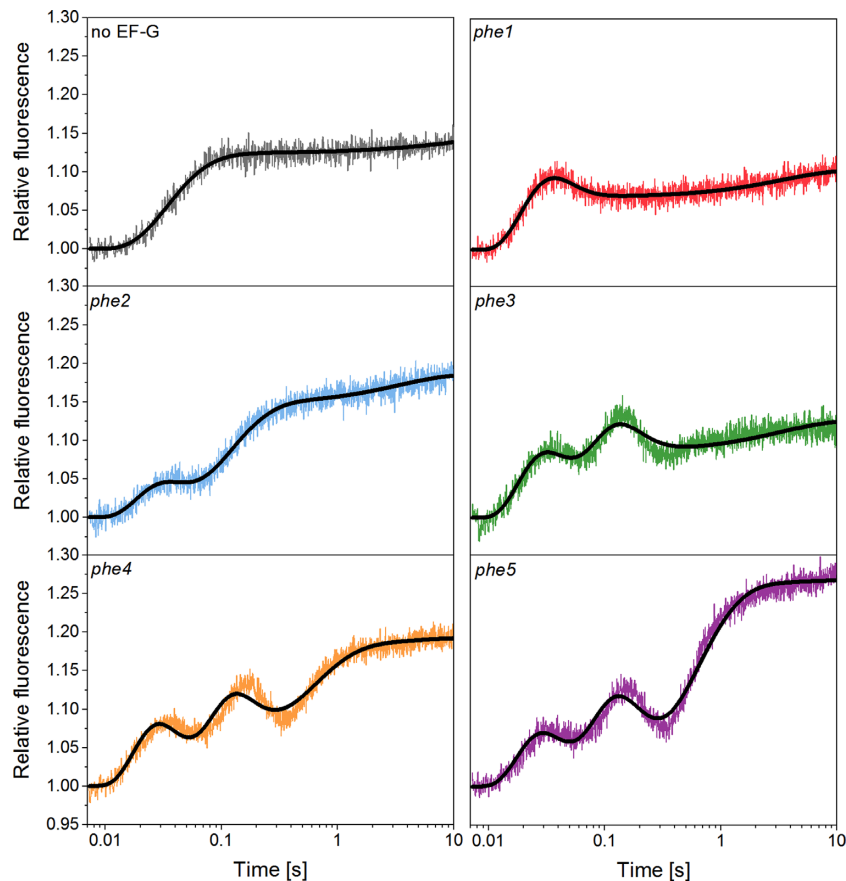


Figure 3. Measured fluorescence signatures of the *in-vitro* synthesis of BOF-fMetPhe_n peptides (colored lines) and best fit in terms of least squares of the theoretical translation model (black lines). The label ‘no EF-G’ indicates translation of poly(U) mRNA in the absence of EF-G.

Table 1. Codon position-specific translation rates calculated from fitted *in-vitro* rates of ribosomal transitions

Codon position	Translation rate [s^{-1}]
First	28 ± 3
Second	9 ± 0.5
Third	20 ± 2
Fourth	2 ± 0.1
Fifth	13 ± 1

translation rates vary by more than one order of magnitude with the highest rates found for the first and the third codon. Compared to the other codons, the translation rate of the fourth codon is strikingly slow. This difference seems surprising because all codons are identical in their nucleotide sequence. A similarly pronounced slow-down during the early phase of translation elongation was observed by (15), who deduced ribosome stalling at the fifth codon position by genome-wide ribosome profiling of eukaryotic cells (15). Stalling at the fourth UUU codon could be a generic feature of the peptide-tunnel, irrespective of the mRNA sequence, as proposed in (15). Further studies with different types of mRNA sequences will be necessary to elucidate the mechanism of early translation elongation pausing, which is beyond the scope of the work presented here.

Ternary complex concentration dependence confirms slow-down at the fourth UUU codon

To further investigate and validate the deduced slow-down at the fourth codon, we measured the fluorescence signatures of *phe4* mRNA translation for four different concentrations X of ternary complexes (EF-Tu-GTP-Phe-tRNA^{Phe}) in the reaction solution, see Figure 4. We compared the experimental fluorescence signatures to those predicted by our model, where we took into account the altered ternary complex concentration X by recalculating the binding rate $\omega_{on} = \kappa_{on}X$ with binding rate constant $\kappa_{on} = 175 \mu M^{-1} s^{-1}$. Apart from the binding rate ω_{on} , we used the same kinetic parameters as before, i.e. no rate fitting was performed here. In all cases, theoretical predictions and experimental data agree well, confirming the low translation rate of $2 s^{-1}$ for the fourth codon.

Computational method detects subtle changes in fluorescence intensities

While traversing the ribosomal exit tunnel, the BOF fluorophore attached to the nascent peptide’s N-terminus probes different chemical environments. Thus, the intensity of the emitted light (IFI) varies with the state of the translation process. As explained above and in the Materials and Methods section, we determine $n + 2$ IFIs for each mea-

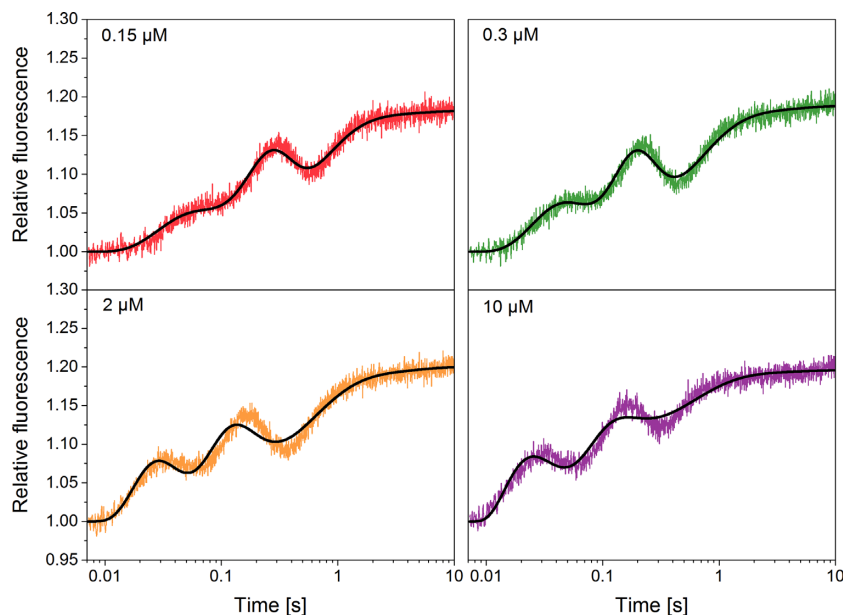


Figure 4. Comparison of experimental (colored lines) and predicted (black lines) fluorescence signatures of *phe4* translation for different ternary complex concentrations.

sured fluorescence signature by our fitting procedure, where n is the number of UUU codons of the mRNA and $n = 0$ in the absence of EF-G. IFIs obtained by fitting the fluorescence signatures of *phe1* to *phe5* translation are shown in Figure 5 A. In addition, we analyzed the variations in fluorescence during the synthesis of BOF-fMetPhe₄ peptides for different ternary complex concentrations. The resulting IFIs can be found in Figure 5 B. Generally, despite variations between the experiments and thermal noise in the fluorescence signatures, the determined IFIs are surprisingly coherent and scatter very little, see Table S5, with a standard deviation of <3%. This deviation is small compared to the differences between the IFIs obtained for the different states of the translation process. Thus, the method presented here is sensitive enough to accurately detect relatively small changes in the IFIs, see Figure 5.

CONCLUSION

Here, we described a method to monitor the progressive motion of a nascent peptide chain through the ribosomal exit tunnel and investigated the kinetics of this process. We used a stopped-flow instrument to study the *in-vitro* synthesis of fMetPhe_n peptides of different lengths that are fluorescence labeled at their N-termini. During translation, the changing environment of the growing peptide and changes in its conformation lead to time-dependent fluorescence signals which represent sequence-specific fluorescence signatures. Because measurements are performed in ensemble, features of the individual fluorescence signatures of each ribosome are blurred because of the stochasticity of the translation process. Thus, total fluorescence signatures obtained from ensemble experiments have to be decomposed mathematically to reveal the hidden information on fluorescence intensities emitted by individual fluorophores and on the kinetics of the individual translation steps. To achieve this de-

composition, we modeled the translation elongation cycle as a codon-specific Markov process as introduced in (19,20), where each transition in the Markov process corresponds to one sub-step of the elongation cycle. Furthermore, each state of the Markov process is related to a specific Intrinsic Fluorescence Intensity (IFI) and transitions between two states are governed by kinetic rates. We determined the IFIs as well as the kinetic rates of the translation process by fitting the theoretical model to a sequence of experimental fluorescence signatures. The method presented here accurately describes the biological process and is sensitive enough to investigate small changes in fluorescence during translation. Thus, this method could also be used to identify sequence-specific IFI patterns and to reveal characteristic sites of nascent chain interactions within the ribosomal exit tunnel. Furthermore, the technique allowed us to gain insight into the dynamics of the translation process. From the deduced kinetic rates, we calculated average position-specific translation rates for the first to the fifth codon. We expected very little variation between these translation rates because all codons in the used poly(U) mRNAs were identical. However, the translation rate of the fourth UUU codon is about an order of magnitude lower than that of the other UUU codons. This observation coincides with a previous experimental finding by (15), who reported ribosome stalling at the fifth codon position seen in genome-wide ribosome profiling data of eukaryotic cells (15). Thus, stalling within the first codons could be a generic feature of the tunnel-peptide interactions irrespective of the mRNA sequence and the source of ribosomes.

The method presented here provides a novel approach for quantitative analyses of ribosomal stalls and pauses occurring during protein synthesis. Therefore, it could prove useful for the interpretation of ribosome profiling data or the study of co-translational folding events. Furthermore, our method could be applied to study the processivity of

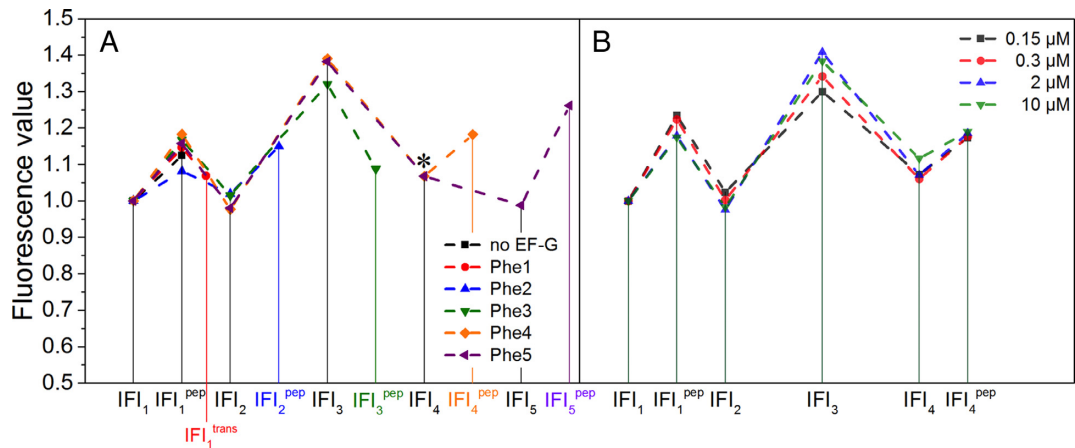


Figure 5. Intrinsic Fluorescence Intensities (IFIs) corresponding to different states of the translation process. The intensities are normalized to the initial value. The IFI corresponding to the end state, which is an off-pathway state, is not shown. (A) IFIs obtained from fluorescence signatures of *phe1* to *phe5* translation. For the fluorescence signature of *phe5* translation, simultaneous fitting of IFI_4 (*) and IFI_5 did not yield a unique solution. Thus, IFI_4 was assumed to have the same value as IFI_4 obtained from fitting the fluorescence signature of *phe4* translation. (B) IFIs obtained from fluorescence signatures of *phe4* translation for different ternary complex concentrations. All IFIs are displayed in Tables S3 and S4 with averages and standard deviations given in Tables S5 and S6 in the Supplementary Information.

other enzymes. For example, processivity and back-tracking of DNA polymerases could be elucidated by an approach analogous to the method presented here.

SUPPLEMENTARY DATA

Supplementary Data are available at NAR Online.

FUNDING

German Science Foundation (Deutsche Forschungsgemeinschaft) via Research Unit FOR 1805. Funding for open access charge: Max Planck Institute of Colloids and Interfaces.

Conflict of interest statement

None declared.

REFERENCES

- Ban, N., Nissen, P., Hansen, J., Moore, P.B. and Steitz, T.A. (2000) The complete atomic structure of the large ribosomal subunit at 2.4 Å resolution. *Science*, **289**, 905–920.
- Lu, J. and Deutsch, C. (2005) Folding zones inside the ribosomal exit tunnel. *Nat. Struct. Mol. Biol.*, **12**, 1123–1129.
- Balchin, D., Hayer-Hartl, M. and Hartl, F.U. (2016) In vivo aspects of protein folding and quality control. *Science*, **353**, aac4354.
- Jacobson, G.N. and Clark, P.L. (2016) Quality over quantity: optimizing co-translational protein folding with non-optimal synonymous codons. *Curr. Opin. Struct. Biol.*, **38**, 102–110.
- Komar, A.A. (2016) The yin and yang of codon usage. *Hum. Mol. Genet.*, **25**, R77–R85.
- O'Brien, E.P., Ciryam, P., Vendruscolo, M. and Dobson, C.M. (2014) Understanding the influence of codon translation rates on cotranslational protein folding. *Acc. Chem. Res.*, **47**, 1536–1544.
- Rodnina, M.V. (2016) The ribosome in action: Tuning of translational efficiency and protein folding. *Protein Sci.*, **25**, 1390–1406.
- Thommen, M., Holtkamp, W. and Rodnina, M.V. (2017) Co-translational protein folding: progress and methods. *Curr. Opin. Struct. Biol.*, **42**, 83–89.
- Ziv, G., Haran, G. and Thirumalai, D. (2005) Ribosome exit tunnel can entropically stabilize alpha-helices. *PNAS*, **102**, 18956–18961.
- Varenne, S., Buc, J., Llobes, R. and Lazdunski, C. (1984) Translation is a non-uniform process: effect of tRNA availability on the rate of elongation of nascent polypeptide chains. *J. Mol. Biol.*, **180**, 549–576.
- Sørensen, M.A. and Pedersen, S. (1991) Absolute in vivo translation rates of individual codons in *Escherichia coli*: the two glutamic acid codons GAA and GAG are translated with a threefold difference in rate. *J. Mol. Biol.*, **222**, 265–280.
- Chaney, J.L. and Clark, P.L. (2015) Roles for synonymous codon usage in protein biogenesis. *Ann. Rev. Biophys.*, **44**, 143–166.
- Chadani, Y., Niwa, T., Chiba, S., Taguchi, H. and Ito, K. (2016) Integrated in vivo and in vitro nascent chain profiling reveals widespread translational pausing. *PNAS*, **113**, E829–E838.
- Wilson, D.N., Arenz, S. and Beckmann, R. (2016) Translation regulation via nascent polypeptide-mediated ribosome stalling. *Curr. Opin. Struct. Biol.*, **37**, 123–133.
- Han, Y., Gao, X., Liu, B., Wan, J., Zhang, X. and Qian, S. (2014) Ribosome profiling reveals sequence-independent post-initiation pausing as a signature of translation. *Cell Res.*, **24**, 842–851.
- Rodnina, M.V. and Wintermeyer, W. (1995) GTP consumption of elongation factor Tu during translation of heteropolymeric mRNAs. *PNAS*, **92**, 1945–1949.
- Rodnina, M.V., Savelsbergh, A., Matassova, N.B., Katunin, V.I., Semenov, Y.P. and Wintermeyer, W. (1999) Thiostrepton inhibits the turnover but not the GTPase of elongation factor G on the ribosome. *PNAS*, **96**, 9586–9590.
- Holtkamp, W., Cunha, C.E., Peske, F., Konevega, A.L., Wintermeyer, W. and Rodnina, M.V. (2014) GTP hydrolysis by EF synchronizes tRNA movement on small and large ribosomal subunits. *EMBO J.*, **33**, 1073–1085.
- Rudorf, S., Thommen, M., Rodnina, M.V. and Lipowsky, R. (2014) Deducing the kinetics of protein synthesis in vivo from the transition rates measured in vitro. *PLoS Comput. Biol.*, **10**, e1003909.
- Rudorf, S. and Lipowsky, R. (2015) Protein synthesis in *E. coli*: dependence of codon-specific elongation on tRNA concentration and codon usage. *PLOS ONE*, **10**, 1–22.
- Wohlgemuth, I., Pohl, C., Mittelstaet, J., Konevega, A.L. and Rodnina, M.V. (2011) Evolutionary optimization of speed and accuracy of decoding on the ribosome. *Phil. Trans. R. Soc. B*, **366**, 2979–2986.
- Belardinelli, R., Sharma, H., Caliskan, N., Cunha, C.E., Peske, F., Wintermeyer, W. and Rodnina, M.V. (2016) Choreography of molecular movements during ribosome progression along mRNA. *Nat. Struct. Mol. Biol.*, **23**, 03.
- Taylor, H.M. and Samuel, K. (1985) *An Introduction to Stochastic Modeling*. Academic Press.